symmetry

MDPI

Article

# A Method to Optimize the Electron Spectrum for Simulating Thermo-Mechanical Response to X-ray Radiation

**Xianwen Ran *, Bo Wang *, Kun Zhang and Wenhui Tang**

College of Liberal Arts and Sciences, National University of Defense Technology, Changsha 410073, China; nudtzhangkun@163.com (K.Z.); tangwenhui@nudt.edu.cn (W.T.)

* Correspondence: ranxianwen@nudt.edu.cn or ranxianwen@163.com (X.R.); wangbo09b@163.com (B.W.); Tel.: +86-135-7415-1246 (X.R.); +86-132-9685-6364 (B.W.)

Received: 7 December 2019; Accepted: 25 December 2019; Published: 27 December 2019


**Abstract:** The X-ray pulse originating from high altitude nuclear detonation (HAND) is mainly soft X-ray and its intensity is high enough to gasify the penetrated material and then lead to the severe thermo-mechanical deformation of unpenetrated material from the gasified blow-off effect. This effect cannot be directly reproduced in a lab for the lack of the X-ray source like HAND. At present, the low-energy relativistic electron beams resulting from an electron accelerator are usually used to approximately reproduce this effect, but the difference in the energy-deposited profile in materials between the electron and X-ray cannot be eliminated. In this paper, the symmetric linear least squares method was used to optimize the electron spectrum, and the general Monte Carlo N-Particle Transport Code calculations showed the optimized spectrum can produce the same energy-deposited profile in aluminum, copper, and tantalum with the soft X-rays like 1 keV or 3 keV spectrums. This indicates that it is possible to simulate the severe thermo-mechanical deformation resulting from HAND using the optimized electron spectrums.

**Keywords:** high altitude nuclear detonation; soft X-ray; thermo-mechanical deformation; least squares method; gasified blow-off effect; energy-deposited profile

## 1. Introduction

When the nuclear bomb explodes over high altitude (more than 80 km to 100 km distance from the ground), the soft X-ray pulse (mainly between 1 keV and 3 keV) resulting from high altitude nuclear detonation (HAND) can propagate undamped for a long distance in the surrounding rarefied air. The intensity of the X-ray pulse is so high that it can gasify all the materials that the X-ray penetrates. The gasified material will adiabatically expand and the subsequent blow-off effect can produce the thermal shock wave propagating into the unpenetrated material. The propagation and reflection of the thermal shock wave can result in severe thermo-mechanical deformation of materials or structures [1–3]. So, some scientists propose to damage spatial objects such as missiles, satellites, and near-earth asteroids with HAND [4–6]. But how to reproduce this physical process experimentally with the facilities in the lab is still a tough problem [7].

In fact, the X-ray pulse duration is short to about 100 ns and then the thermo-mechanical deformation can merely be determined by the energy-deposited profile in the material [8–10]. If two radiations have the same energy-deposited profiles in the same material, they will lead to the same thermo-mechanical deformation [11–13]. Unfortunately, it is hard to find one radiation in the lab which can produce the same energy-deposited profiles as that of HAND. At present, the low-energy relativistic electron beams resulting from an electron accelerator are usually used to simulate the

thermo-mechanical deformation resulting from HAND, though the differences in the energy-deposited profiles exist. So, at the lack of X-ray sources such as HAND, it is key to find the electron spectrum that can reproduce the same energy-deposited profile as HAND. In this paper, one symmetric linear least squares method is proposed to optimize the electron beam spectrum, and through the calculations with MCNP software (a general Monte Carlo N-Particle Transport Code, MCNP) [14], the optimized electron beam spectrum can produce the same energy-deposited profiles as the 1 keV and 3 keV X-rays do.

## 2. The Optimized Method

### *2.1. The Differences between X-ray and Electron Interaction with Materials*

The deposited-energy profiles of X-ray and electron in the same material are merely determined by their mean free paths in that material, which are usually different for their different physical mechanisms of interaction with material. The X-ray pulse of HAND can be treated as a black body spectrum which is defined with a characteristic temperature. Figure 1 shows the energy-deposited profiles in aluminum of 3 keV X-ray and electron of one certain energy with the same energy fluence. We can see that the deposited energy per gram resulting from 3 keV X-ray radiation declines quickly with the increase of energy-deposited depth, while the electron has a greater energy-penetrated depth and its energy-deposited profile rises first and then goes down, which means that the profile has an obvious peak point. If using this electron spectrum to simulate the thermo-mechanical response resulting from HAND, the experimental results cannot be used to assess that resulted from HAND. So, it is necessary to optimize the electron spectrum to get the electron spectrum that can be used to simulate the thermo-mechanical response resulted from HAND.

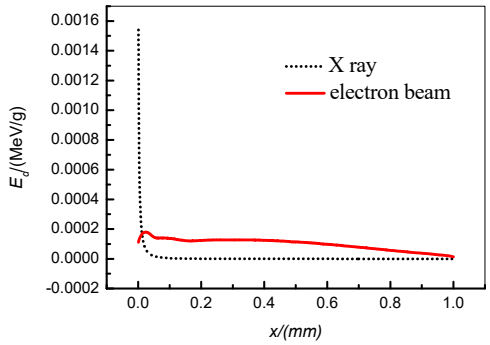


**Figure 1.** The energy-deposited profiles of electron beam and X-ray of the same energy fluence in aluminum.

To explore the feasibility of optimizing the electron spectrum, we presented the energy-deposited profiles of electrons of different energy in Figure 2. We can see, the lower the electron energy is, the closer the peak point is to the radiating surface, which indicates that it is more suitable to use the low-energy electrons to simulate the thermo-mechanical response resulted from HAND.

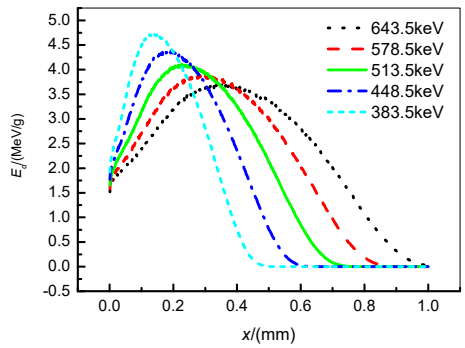


**Figure 2.** The energy-deposited profiles in aluminum of electrons of different energy.

### 2.2. The Optimized Method for Electrons

The electron spectrum used to simulate the thermo-mechanical response must have the same energy fluence and the same energy-deposited profile in the material as that of X-ray. So, the optimized method needs to satisfy the following preconditions:

(i) Assuming this problem is in one dimension;

(ii) Dividing the material into $N$ parts along the radiated direction and as shown in Equation (1), in each part, the deposited energy from the electron should be correspondingly equal to that from the X-ray

$$e_i^p = e_i^e i = 1, 2, \cdots, n \tag{1}$$

where, the superscripts $p$ and $e$ denote X-ray and electron respectively, subscript $i$ denotes the order of the part;

(iii) Assuming the electron spectrum is continuous and has a maximum energy per electron $e_{\max}$, and the minimum is zero (Figure 3). The energy span of the whole electron spectrum is divided into $m$ energy bins, and in the $j$th energy bin, the midpoint value of the energy per electron is $e_j$ ($j$ = 1, 2, . . . , $m$), the total number of electrons is $a_j$ ($j$ = 1, 2, . . . , $m$). This means the continuous spectrum has been changed to a discrete spectrum (see Figure 4). The optimization purpose is to get the number of electrons $a_j$ in each energy bin;

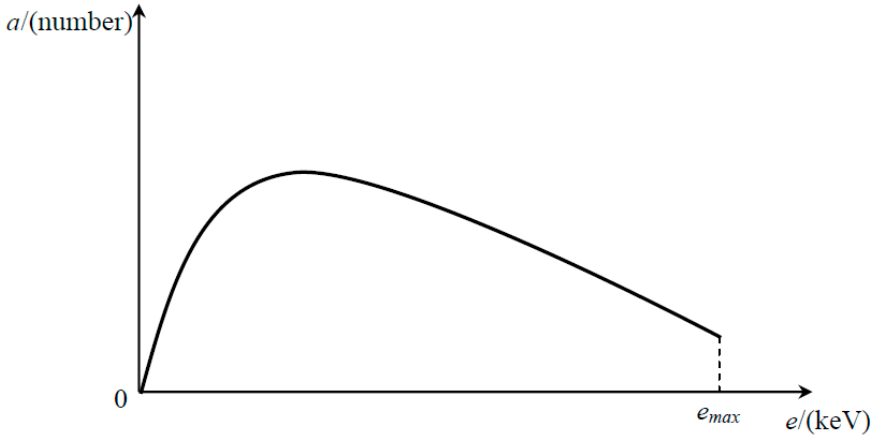


**Figure 3.** The continuous spectrum of electrons.

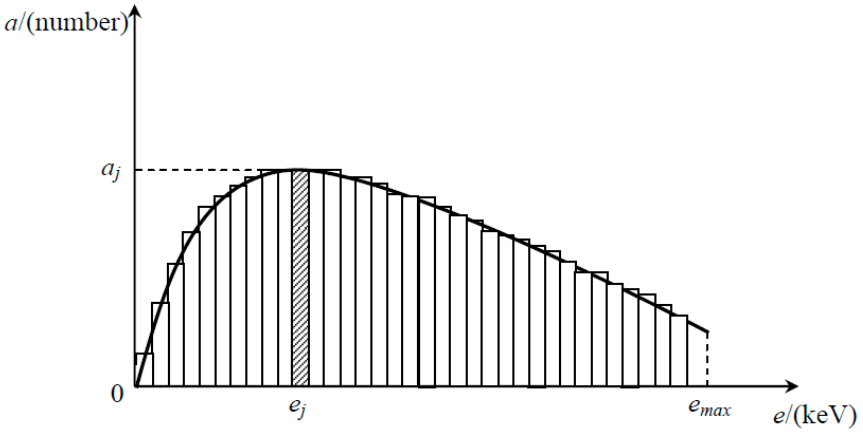


**Figure 4.** The discrete spectrum of electrons.

(iv) The deposited energy from electrons in the $i$th part of material is $e_i^e$, and for one electron in the $j$th energy bin (which means the electron has the energy $e_j$), the deposited energy in the $i$th part is $e_{ij}$ which can be calculated with the MCNP software.

According to the above preconditions, the deposited energy in the $i$th part result from the electron spectrum can be calculated with the following Equation (2).

$$e_i^e = \sum_{j=1}^{m} e_{ij} a_j \tag{2}$$

The energy-deposited profile in the material that resulted from X-ray with a certain energy fluence can also be calculated with MCNP software, which means the deposited energy $e_i^p$ in each part is known. Combining the Equations (1) and (2), we can have the following matrix representation:

$$\mathbf{D} = \mathbf{E} \cdot \mathbf{A} \tag{3}$$

where the matrixes **D**, **E**, and **A** have the form as those in the Equation (4).

$$\mathbf{D} = \begin{pmatrix} e_1^p \\ e_2^p \\ \vdots \\ e_n^p \end{pmatrix} \mathbf{E} = \begin{pmatrix} e_{11} & e_{12} & \cdots & e_{1m} \\ e_{21} & e_{22} & \cdots & e_{2m} \\ \vdots & \vdots & \ddots & \vdots \\ e_{n1} & e_{n2} & \cdots & e_{nm} \end{pmatrix} \mathbf{A} = \begin{pmatrix} a_1 \\ a_2 \\ \vdots \\ a_m \end{pmatrix} \tag{4}$$

In addition, the number of electrons in each energy bin cannot be negative, that is

$$a_j \geq 0 \tag{5}$$

Now, the problem has changed to how to solve the Equation (3) to have the solution **A**. According to the linear algebra, the Equation (3) has $m - n + 1$ sets of solutions if $n < m$; and has only one set of solutions if $n = m$. If $n > m$, the Equation (3) has no solution but one approximated solution.

According to the optimization theory, this approximated solution can be gotten with the least squares method under constraints. That is to find the minimum value

$$\min(\|\mathbf{E} \cdot \mathbf{A} - \mathbf{D}\|)^2 \tag{6}$$

The matrix **A**, which satisfied the Equation (6), can tell us how to distribute the electron numbers in each energy bin, and together with $m$ energy bins was exactly the optimized electron spectrum that we want.

## 3. Specific Results

To show the validity of the optimization method above, the electron spectrum was divided into 50 energy bins with the energy span from 6.5 keV to 643.5 keV. The material was divided into 1000 parts. With the software MCNP, for the electron with the energy $e_j$, the energy depositing in the $i$th part results can be calculated in advance for a specific material, that is, the value $e_{ij}$ has been known before optimization. The spectrum to be simulated is 1 keV and 3 keV X-ray spectrum with the energy fluence w = 200 J/cm$^2$ and 300 J/cm$^2$.

### *3.1. The effect of X-ray spectrum*

Taking the aluminum as the example, the optimization for 1 keV and 3 keV X-ray spectrums with the energy fluence 300 J/cm$^2$ was accomplished, and the optimized results are shown in the Figures 5 and 6.

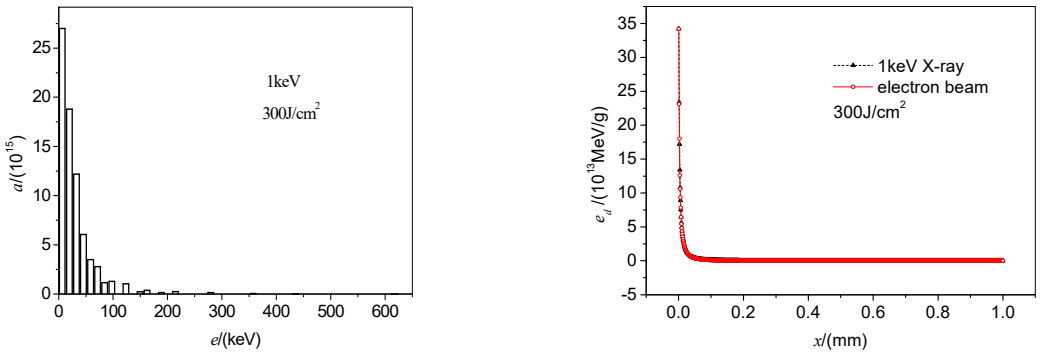


(**a**) (**b**)

**Figure 5.** The optimized results for 1 keV X-ray with fluence 300 J/cm$^2$. (**a**) The electron spectrum after optimization; (**b**) Comparison of the energy-deposited profiles between X-ray and electron.

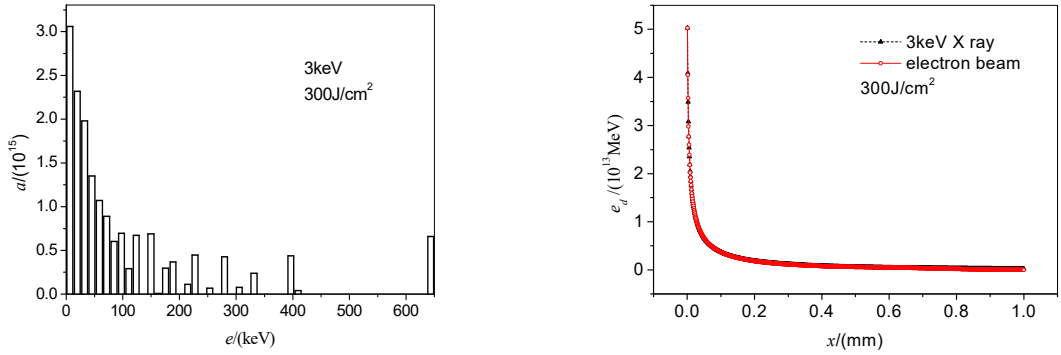


(**a**) (**b**)

**Figure 6.** The optimized results for 3 keV X-ray with fluence 300 J/cm$^2$. (**a**) The electron spectrum after optimization; (**b**) Comparison of the energy-deposited profiles between X-ray and electron.

From Figures 5b and 6b, we can see that the energy-deposited profiles after optimization agreed well with that of X-rays. But the electron spectrums after optimization for 1 keV X-ray are completely different from that for 3 keV X-ray as shown in Figures 5a and 6a. In the electron spectrum for 1 keV X-ray, the number of electrons with low energy is less than that for 3 keV X-ray. Which indicates, once again, that the electrons with low energy are appropriate to be used to simulate the soft X-ray.

If the fluence of X-ray was changed to 200 J/cm$^2$, the optimized results are shown in Figures 7 and 8. From the comparison of Figures 5 and 6 with Figures 7 and 8, we can see that the electron spectrum after optimization does not change but the number varies which means the fluence is merely related with the number of electrons. In other words, the optimization method presented here can be applied to X-ray with any fluence by only changing the number of electrons.

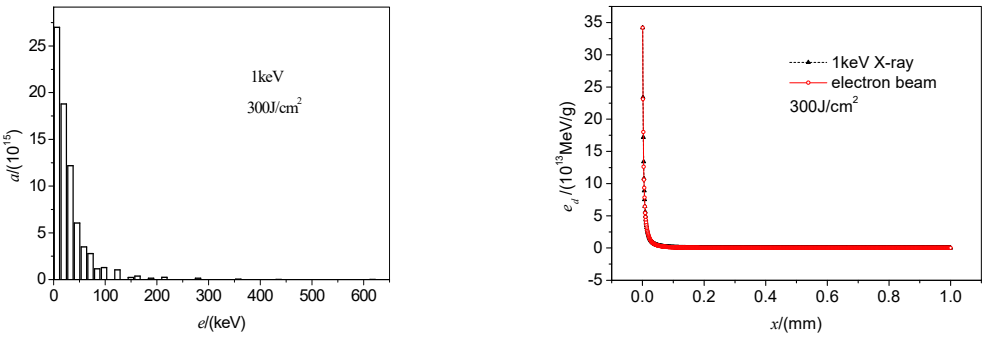


(**a**) (**b**)

**Figure 7.** The optimized results for 1 keV X-ray with fluence 200 J/cm$^2$. (**a**) The electron spectrum after optimization; (**b**) Comparison of the energy-deposited profiles between X-ray and electron.

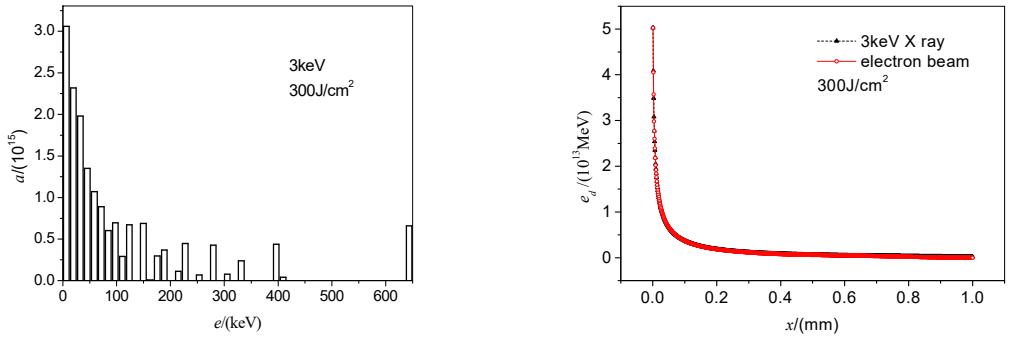


(**a**) (**b**)

**Figure 8.** The optimized results for 3 keV X-ray with fluence 200 J/cm$^2$. (**a**) The electron spectrum after optimization; (**b**) Comparison of the energy-deposited profiles between X-ray and electron.

### *3.2. The Effect of Material*

In nuclear physical theory, except for the density, the energy-deposited profiles resulting from X-rays are merely related to the atomic number $Z$ of the material. So, we take the low-$Z$ material Al, medium-$Z$ material Cu, and high-$Z$ material Ta to test the validity of the optimization method presented here. The X-ray spectrums chosen to be simulated were still 1 keV and 3 keV X-ray. The calculated results are shown in Figures 9 and 10.

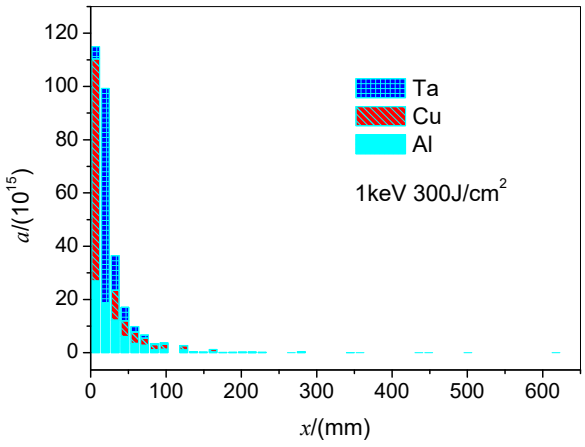


**Figure 9.** Comparison of the electron spectrums used to simulate 1 keV X-ray in three materials: aluminum, copper, and tantalum.

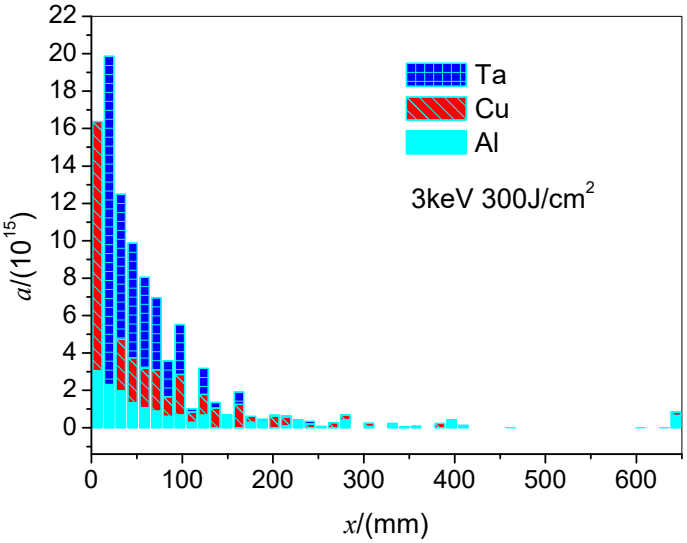


**Figure 10.** Comparison of the electron spectrums used to simulate 3 keV X-ray in three materials aluminum, copper and tantalum.

Figures 9 and 10 show that, after optimization, the electron spectrums varied greatly with materials for the same X-ray. For the electron spectrum for simulating the soft X-ray, the differences among three materials were mainly on the low-energy span; while for the electron spectrum for simulating the hard X-ray, the differences among three materials appeared on all the energy spans. For the high-*Z* material tantalum and the soft X-ray 1 keV, there are more electrons in the low-energy span of the electron spectrum than the electron spectrums for the low-Z material aluminum and the hard X-ray 3 keV. The optimized electron spectrums for three materials also indicate that the optimization method is applicable for all the material no matter which is low-*Z*, medium-*Z*, and high-*Z*.

## 4. Conclusions

In the paper, one optimization method was presented to optimize the electron spectrum which was used to simulate the thermo-mechanical response of one material resulting from X-ray radiation. The calculated results showed that:

(i) In a material, the electron spectrum after optimization can lead to the same energy-deposited profile that the X-ray spectrum produced; so, if one electron accelerator can adjust the electron spectrum it produced to the optimized one, this accelerator can be used to simulate the thermo-mechanical response resulted from HAND.

(ii) The electron distribution in the optimized electron spectrum was greatly affected by the radiated material and the X-ray spectrum, and the variation in the X-ray fluence would not affect the structure of the optimized electron spectrum but the number of electrons in each energy bin.

It should be mentioned that, at present, the scientists are unable to find a way to control precisely the energy and the speed of the numerous electrons emitting from accelerators, so it is still a tough task to realize this optimizing method on electron accelerators.

**Author Contributions:** Conceptualization, X.R.; methodology, K.Z.; validation, B.W. and X.R.; formal analysis, X.R.; resources, B.W.; data curation, B.W.; Writing—Original draft preparation, X.R.; Writing—Review and editing, X.R.; supervision, X.R.; and project administration, W.T. All authors have read and agreed to the published version of the manuscript.

**Funding:** This research was funded by the National Natural Science Foundation of China (grant Nos. 11002162 and 11072262). The financial contributions are gratefully acknowledged.

**Conflicts of Interest:** The authors declare no conflict of interest.

## References


1. Doron, K.; Eli, W. Hard X-ray Emission from Accretion Shocks around Galaxy Clusters. *J. Cosmol. Astropart. Phys.* **2010**, *25*, 1–14.
2. George, R.S.; David, H.M.; Hani, K. Radioisotope electric propulsion (REP): A near-term approach to nuclear propulsion. *Acta Astronaut.* **2010**, *7*, 501–507.
3. Andreas, B.; Bernd, S.; Martin, B.K. Introduction to the Topical Volume: Recent Advances in Nuclear Explosion Monitoring. *Pure Appl. Geophys.* **2010**, *7*, 373–379.
4. Lomov, I.; Herbold, E.B.; Antoun, T.H. Influence of mechanical properties relevant to standoff deflection of hazardous asteroids. *Procedia Eng.* **2013**, *58*, 251–259. [CrossRef]
5. Hammerling, P.; Remo, J.L. NEO interaction with nuclear radiation. *Acta Astronaut.* **1995**, *36*, 337–346. [CrossRef]
6. Holsapple, K.A. About deflecting asteroids and comets. *Mitig. Hazard. Comets Asteroids* **2004**, 113–140.
7. Qiu, A.C.; Zhang, J.S.; Peng, J.C. Research progress about high power pulse ion beam of imitating X-ray thermal-mechanical response. *Nucl. Technol.* **2002**, *36*, 714–719.
8. Yang, H.L.; Qiu, A.C.; Zhang, J.S. Simulation calculation for the energy deposition profile and the transmission fraction of intense pulsed electron beam at various incident angles. *High Power Laser Part. Beams* **2002**, *14*, 778–782.
9. Jane, L.; Fox, M.I.; Galand, R.E. Energy deposition in planetary atmospheres by charged particles and solar photons. *Space Sci. Rev.* **2008**, *39*, 213–220.
10. Mihailo, D.R.; Dragan, D.M. Laser beam spatial profile determination by pulsed photoacoustics: Exact solution. *Meas. Sci. Technol.* **2010**, *21*, 065603.
11. Lai, D.G.; Zhang, Y.M.; Li, J.X. Design of bremsstrahlung composite thin converter for high current electron beams. *High Power Laser Part. Beams* **2013**, *25*, 1396–1400.
12. Wang, J.G.; Niu, S.L. *Handbook for the Parameters of High-Altitude Nuclear Explosion Effects*, 1st ed.; Atomic Energy Press: Beijing, China, 2010; pp. 45–55.
13. Hu, L.; Lei, Y.; Zhu, J. Simulation on distributed target material impacted by high intensity current multi-pulse electron beam. *High Power Laser Part. Beams* **2013**, *25*, 2125–2129.
14. Esam, M.A.H. Monte Carlo Particle Transport with the MCNP Code. Ph.D. Thesis, University of New Brunswick, Fredericton, NB, Canada, 2011; pp. 1–57.